

UDK 669.018, 676.017.2, 676.017.5

Characterization of FeCoV Alloy Processed by PIM/MIM Route

Borivoje Nedeljković¹, Nebojša Mitrović¹, Jelena Orelj¹, Nina Obradović², Vladimir Pavlović²

¹Joint Laboratory for Advanced Materials of SASA, Section for Amorphous Systems, Faculty of Technical Sciences Čačak, Svetog Save 65, 32000 Čačak, University of Kragujevac, Serbia

²Institute of Technical Sciences of SASA, Knez Mihailova 35, 11000 Belgrade, Serbia

Abstract:

In this study the characterization of FeCo-2V alloys toroidal samples produced by PIM/MIM technology was presented. The feedstock for metal injection molding (MIM) was prepared by mixing starting FeCoV powder with a low viscosity binder. Green samples were subjected to solvent debinding and subsequent thermal debinding followed by sintering. Sintering was performed during 3.5 hours from 1370 °C to 1460 °C in hydrogen atmosphere in order to attain the appropriate mechanical and magnetic properties.

Microstructure, hardness HV10 and magnetic hysteresis B(H) were investigated as a function of sintering temperature. Optimum combination of functional properties was observed after sintering at temperature of 1370 °C. In addition, magnetic properties were analyzed as frequency dependent and successfully simulated in operating frequency range from 5 Hz to 60 Hz.

Keywords: Powder injection moulding technology; FeCoV alloy; Structural properties; Mechanical properties; Magnetic properties.

1. Introduction

Powder injection moulding (acronym PIM) is technology that can offer very efficient manufacturing of ceramic or metallic parts with complex geometries [1-4]. Materials that contain metal elements were produced by variation of PIM technology named metal injection molding (MIM). MIM as well as direct laser metal sintering (DLMS) process (where mixed metal powders are consolidated by laser in a single production step [5, 6]) are today very useful technologies for commercial production plenty of magnetic elements. Due to combinations of powders mixture, binders, molding techniques, debinding parameters and sintering temperature/time profiles, PIM technology is more suitable for magnetic materials industry as it enables easier production of complex cores compared to the classical routes [7-9]. Mechanochemical processing of nanostructured Fe₄₉Co₄₉V₂ alloy [10, 11] as well as different composite preparation [12-13] resulted in very specific magnetic properties.

Silva et al [8] investigated equiatomic Fe₅₀Co₅₀ alloy produced by PIM without V addition and concluded that the elimination of vanadium can improve magnetic properties (an increase in relative magnetic permeability at f=0.05 Hz) and contribute to substantial decrease in sintering temperature (980 °C instead of common sintering temperature of 1330 °C).

*) Corresponding author: nebojsa.mitrovic@ftn.kg.ac.rs

Microstructure of the V added alloy exhibits smaller grain size with increased porosity as a main obstacles for magnetic domains movement resulting in the magnetic hardening. However, there is no data about mechanical characterization of the PIM samples without vanadium, as the FeCo alloys are very brittle [14]. The vanadium addition up to 2 % wt. improves strength and ductility. In order to successfully prepare functional material for applications it is necessary to perform both mechanical and magnetic characterization.

Advanced soft magnetic materials should exhibit a high saturation magnetic induction B_S and relative magnetic permeability μ_r as well as low core losses and coercive force H_C . High Curie temperature T_C , corrosion resistance and good mechanical properties are also very important for some applications. Iron-cobalt based alloys exhibit unique combination of high B_S and T_C as well as high corrosion resistance [14-16]. The semi-hard magnetic alloy FeCo-2V is widely used in electronics and automation and many of these parts are with complex shapes. Therefore, ferromagnetic parts for high temperature applications can be cost-effectively produced as FeCoV alloys by PIM/MIM route.

2. Experimental

In this work the feedstock was prepared by mixing the starting powder with a Solvent system. The powder was originally prepared for the pressing technology. The feedstock was prepared from very fine powder and binder system that is easily removable by solvent and thermal debinding.

The investigated samples were produced by a Battenfeld HM 600/130 hydraulic drive injection moulding machine. A green cylindrical component with a central hole was prepared in the following dimensions: 10 mm internal diameter, 18 mm external diameter and 28 mm length. The powder injection moulding parameters applied during preparation are given in Table I.

Tab. I Metal injection moulding parameters.

PIM parameter		
Injection temperature	[°C]	150
Tool temperature	[°C]	35
Back pressure	[MPa]	6
Flow rate	[cm ³ /s]	5
Injection pressure	[MPa]	90
Holding pressure	[MPa]	70
Holding time	[s]	4
Filling time	[s]	2
Cooling time	[s]	40

The injected green samples of toroidal shape were first subjected to solvent debinding and subsequent thermal debinding followed by sintering. The applied sintering procedure and atmosphere were taken from the classical procedure with pressed samples with a small modification of the initial stage of sintering to include thermal debinding. Secondary thermal debinding at optimized temperatures (up to 800 °C) and sintering in the temperature range 1370 °C - 1460 °C were performed in a hydrogen atmosphere with a holding time of 3.5 h.

After these thermal processing the obtained samples had internal diameter of 8.5 mm and external diameter of 16 mm. Samples about 7.5 mm high were cut from the centre section of the sintered piece, in order to achieve better measurement accuracy. Magnetic properties on toroidal core samples were measured at room temperature by hysteresis graph Brockhaus

Tester MPG 100 D for soft magnetic materials. The main properties such as remanent induction B_r , coercive force H_c , saturation induction B_s , and relative magnetic permeability μ_r were determined from B-H loops. Maximum excitation was $H_m=10$ kA/m and frequency $f = 60$ Hz. Intrinsic coercivity H_{cJ} was measured by Foerster Koerzimat.

X-ray diffraction patterns of the samples after sintering were obtained using a Philips PW 1050 diffractometer with $\lambda_{CuK\alpha}$ radiation (0.154 nm) and a step/time scan mode of 0.05°/1s. Vickers hardness tests HV_{10} ($F = 98,1$ N) were performed on Reichert measurement equipment. Scanning electron microscopy SEM JSM-6390 LV JEOL was used for microstructural characterization of the investigated samples after sintering process.

3. Results and discussion

The XRD patterns of FeCo-2V alloy samples sintered from 1370 °C to 1460 °C in hydrogen atmosphere are given in Fig. 1. One can see clear evidence of the α -FeCo crystalline phase by main diffraction peak around $2\theta = 45^\circ$ that is found for all investigated samples. An increase of sintering temperature is also followed by more intensive diffraction peaks that is especially evidenced on patterns 1.c and 1.d for samples sintered at 1430 °C and 1460 °C, respectively.

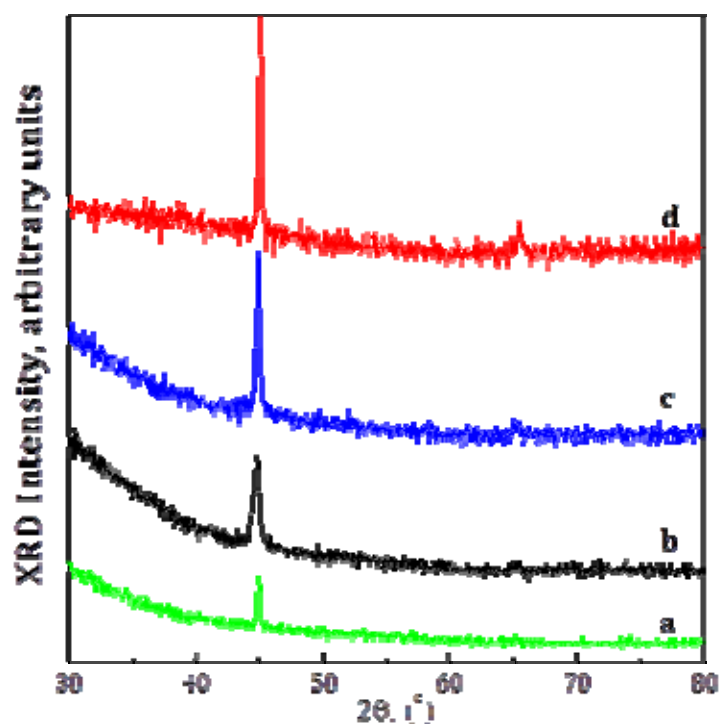


Fig. 1. The XRD patterns of FeCo-2V alloy samples sintered at a) 1370 °C b) 1400 °C, c) 1430 °C and d) 1460 °C in hydrogen atmosphere.

The SEM micrographs obtained from the surface of sintered samples are shown in Fig. 2. It can be seen that the powder particles were melted proportionally to the sintering temperature in the range from 1370 °C to 1430 °C (Figs. 2.a, 2.b and 2.c).

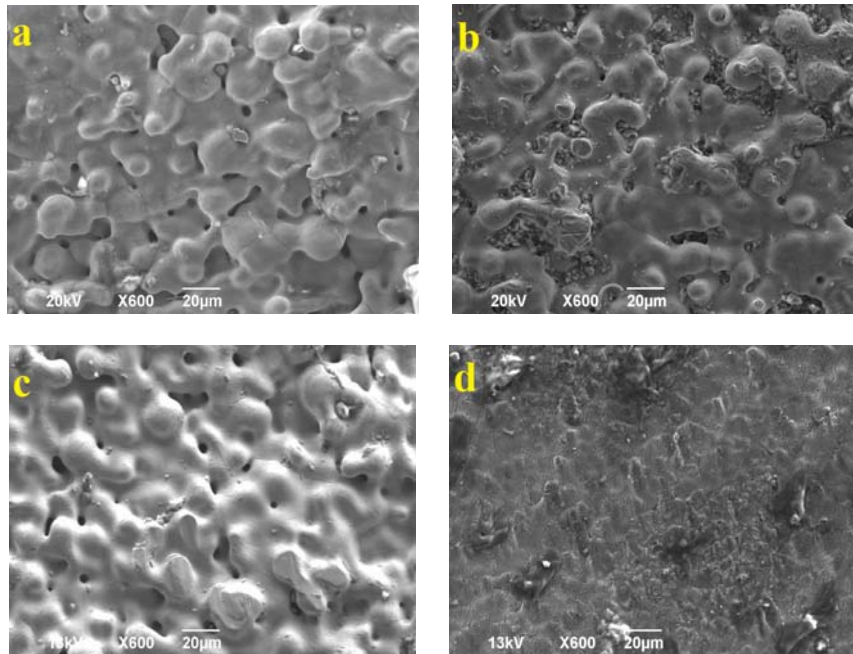


Fig. 2. Microstructures of FeCo-2V alloy samples sintered at a) 1370 °C, b) 1400 °C, c) 1430 °C and d) 1460 °C in hydrogen atmosphere.

The picture of the sample sintered at the highest temperature 1460 °C clearly shows that the particles were completely melted. This is in good correlation with XRD pattern in Fig 1d which exhibits the most intensive crystallization.

Fig. 3 presents the results of the hardness HV_{10} measurements of the investigated sintered samples. The lowest hardness HV_{10} was observed for sample sintered at 1400 °C with value of 262. The substantial increase in sintering temperature is followed by constant increase in hardness, until to the value of 348 for sample sintered at 1460 °C.

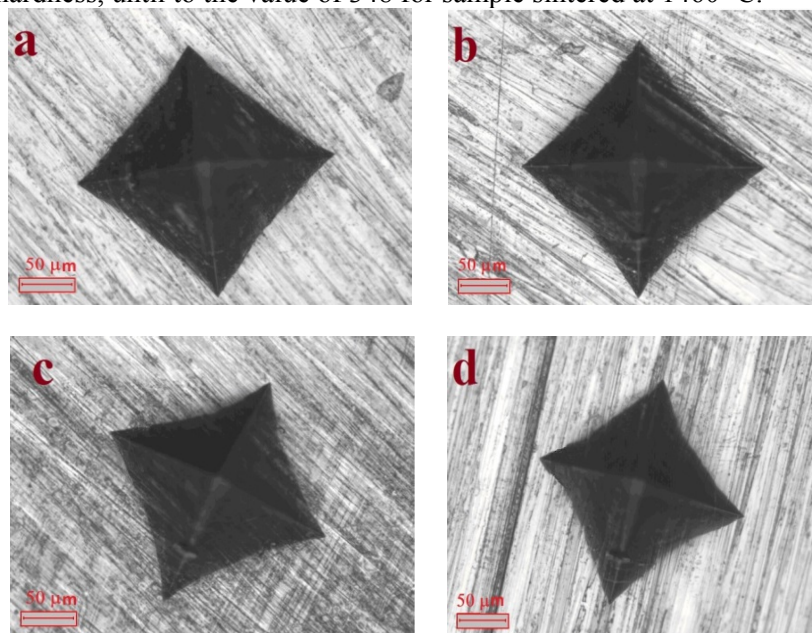


Fig. 3. Hardness HV_{10} of FeCo-2V alloy samples sintered at a) 1370 °C b) 1400 °C, c) 1430 °C and d) 1460 °C in hydrogen atmosphere.

In Fig.4 the mechanical hardness is plotted in correlation with intrinsic coercivity H_{cJ} as a function of the sintering temperature. It is observed that the mechanical hardness does not coincide with the magnetic hardness, i.e. the material with the highest HV10 shows the lowest coercive force H_{cJ} (about 18.4 Oe). This result can be explained as follows.

Magnetic softness is associated with the easy movement of the Bloch walls, i.e. in the structure of the materials there are no plenty of magnetic obstacles that prevent easy movement of magnetic domain walls (“pinning” effect). However, for mechanical hardness the movement of dislocations, i.e. the prevention of this movement, is crucial [17]. That means, the elements in microstructure are highly efficient in blocking the movement of dislocations (associated with the increase in HV10), but not that of the Bloch walls (leading to the decrease in H_{cJ}).

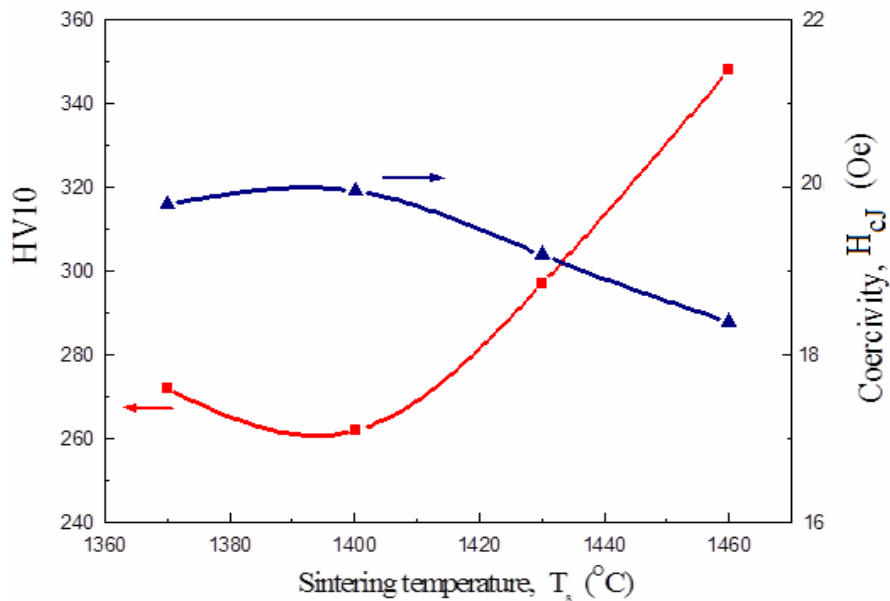


Fig. 4. Hardness HV10 and intrinsic coercivity H_{cJ} of FeCo-2V sintered samples as a function of the sintering temperature.

Similar observation between magnetic and mechanical properties was observed with sintered Fe-Co-Mo/W precipitation hardened alloys and explained with the dislocation dimensions [18]. This result is excellent, as the application of this magnetic material is usually associated with hard mechanical exploitation conditions in magnetic devices like magnetic valves and some magnetic sensors.

Finally, the results of the magnetic measurements are as follows. Fig. 5 presents the families of $B(H)$ hysteresis loops for FeCo-2V alloy sample sintered at different temperatures for the most common exploitation frequency of 50 Hz. It can be noticed clear decrease in the value of magnetic induction B_{10} (attained at the maximum excitation of $H_m = 10$ kA/m) with an increase of sintering temperature due to the harder rotation of magnetization vector inside the magnetic domains as a result of high crystal anisotropy [19]. XRD patterns in Fig. 1 reveals more intensive crystallization with an increase of sintering temperature, and therefore one can expect the increase in crystal anisotropy.

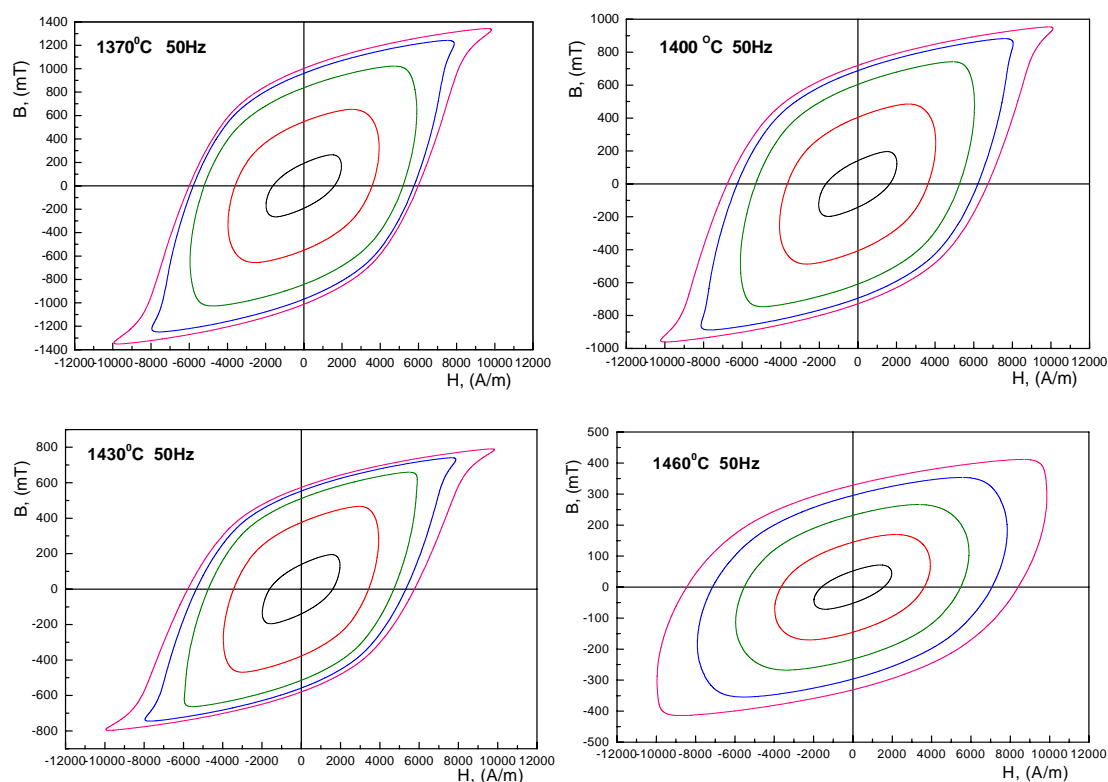


Fig. 5. The families of B(H) hysteresis loops for FeCo-2V alloy samples sintered at different temperatures and at frequency of 50 Hz up to $H_m = 10$ kA/m.

It is well known that an increase in frequency leads to an increase in power losses of magnetic materials [20, 21]. In that sense experiments with the decrease in frequency down to 5 Hz were performed. The families of B(H) hysteresis loops for FeCo-2V alloy sample sintered at 1370 °C and 5 Hz were shown in Fig. 6a, representing the classical R-shape of hysteresis curve for major loop at maximum excitation of $H_m = 10$ kA/m. Similar experiments were performed for all investigated samples at frequencies of 5 Hz, 20 Hz and 50 Hz with the following analysis. Hysteresis loops obtained by increasing excitation were used for estimation dependence of relative permeability μ_r vs. magnetic field H. For the sample sintered at 1370 °C and frequency $f = 5$ Hz it can be observed that the maximum of about $\mu_r \approx 210$ at excitation of 3 kA/m is followed by a constant decrease up to $\mu_r \approx 110$ at excitation of 10 kA/m (see Fig. 6b). Operating frequency of 50 Hz almost halves the maximum of relative permeability to $\mu_r \approx 130$ and shift optimum excitation to the 6 kA/m. The constant increase in sintering temperature is followed by substantial decrease in relative permeability μ_r , until the maximum value of only about 65 was registered for the sample sintered at 1460 °C as it is shown in Fig. 6c.

Nowadays it is necessary to simulate electronic circuits by computer software with option to model magnetic components prepared by variety of soft, semi-hard as well as hard magnetic materials. Programs should also have the capability to simulate frequency dependent hysteresis loops of magnetic materials due to very high operating frequencies in some applications [22]. The most widespread simulation computer software for electronic circuit analysis – PSPICE program uses the Jiles-Atherton model for ferromagnetic hysteresis [23]. This model successfully simulates effects of thermally dependent characteristics of magnetic cores [24]. However, it is approved that the Jiles-Atherton theory of anhysteretic and hysteretic magnetization didn't give correct frequency dependent modelling [25]. Recently,

dynamic loss inclusion in the Jiles–Atherton hysteresis model using the field separation approach has been published [26].

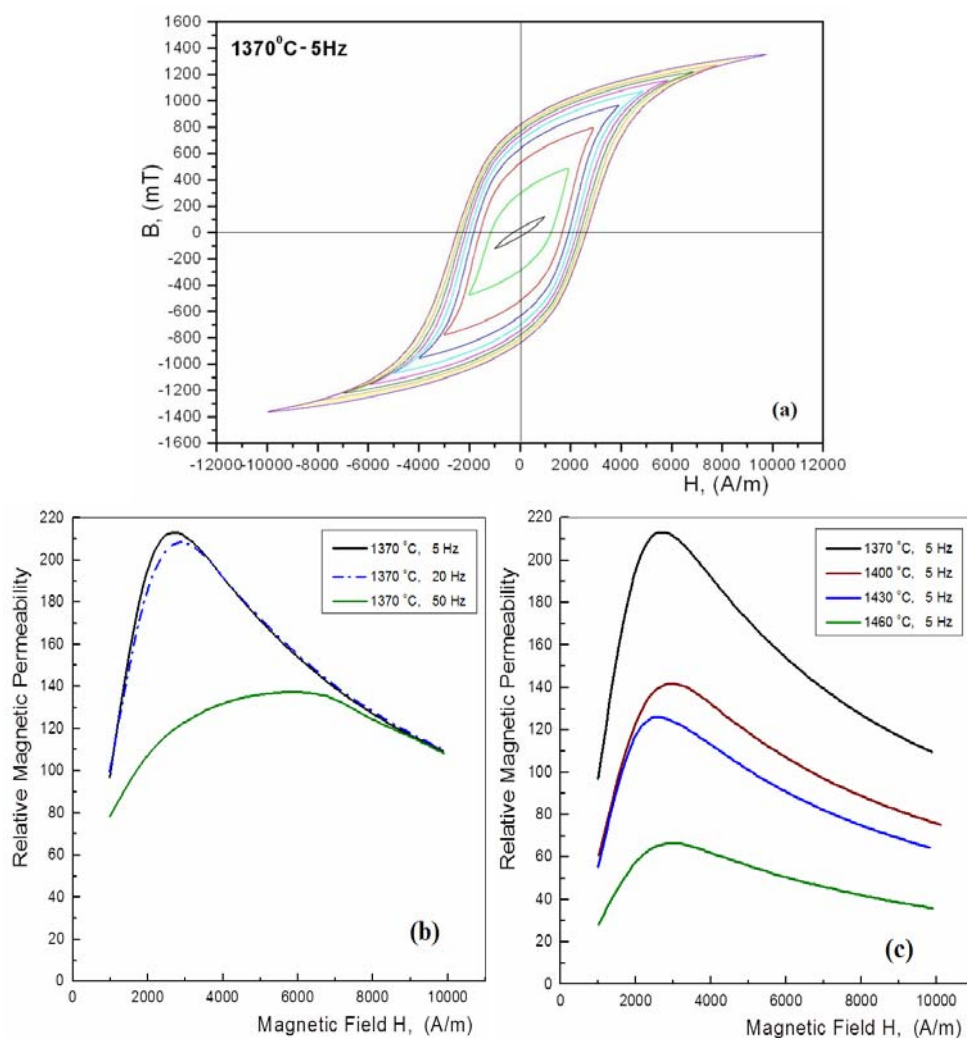


Fig. 6. a) The families of $B(H)$ hysteresis loops for FeCo-2V alloy sample sintered at 1370 °C and 5 Hz, and relative magnetic permeability μ_r vs. magnetic field H , b) for sample sintered at 1370 °C for frequencies 5 Hz, 20 Hz and 50 Hz.; c) for samples sintered at different temperatures for the same frequency of 5 Hz.

In order to model frequency dependent hysteresis loops correctly it is necessary to have real loops obtained by measurements performed on toroidal magnetic core of the investigated material. After modelling numerical data of particular real loops one can have analytical i.e. simulated curves that can be usable for synthesis and testing of electronic devices.

Therefore, in this study mathematical modelling of the FeCo-2V measured hysteresis loops was done by LabVIEW program. Considering that the hysteresis loop has sigmoid shape it is convenient to use arctangent function for its modelling. A new mathematical model for representing ascending and descending branch of hysteresis curve was exploited [27]. Fig. 7 shows measured and modeled families of $B(H)$ hysteresis loops for the sample sintered at 1370 °C obtained at frequency of 5 Hz.

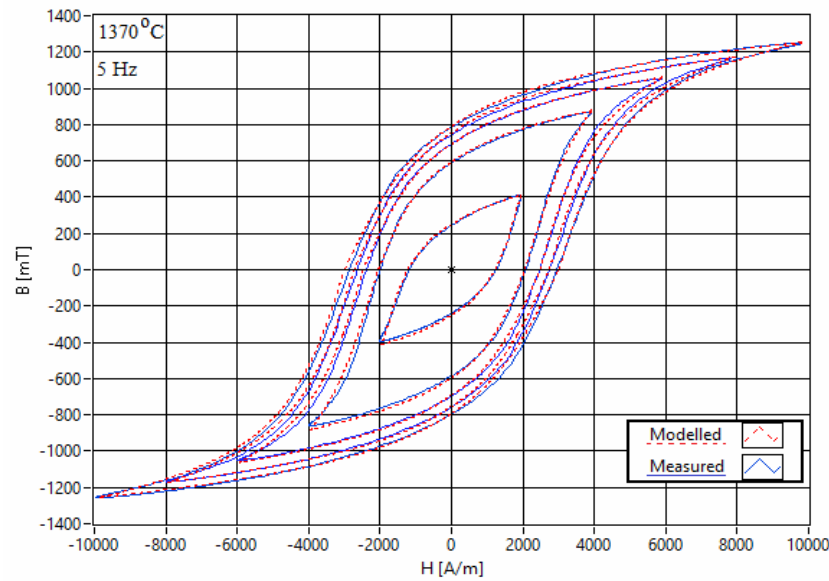


Fig. 7. The families of B(H) hysteresis loops for FeCo-2V sample sintered at 1370 °C obtained at frequency of 5 Hz, measured (line) and modelled (dotted) curves.

It is clear that all minor curves as well as major curve have excellent correlation between the measured and simulated waveforms. The simulation correctly follows hysteresis loops broadening due to the increase in operating frequency from 5 Hz to 60 Hz, as well as anomalous shapes of these dynamic loops (see Fig. 8).

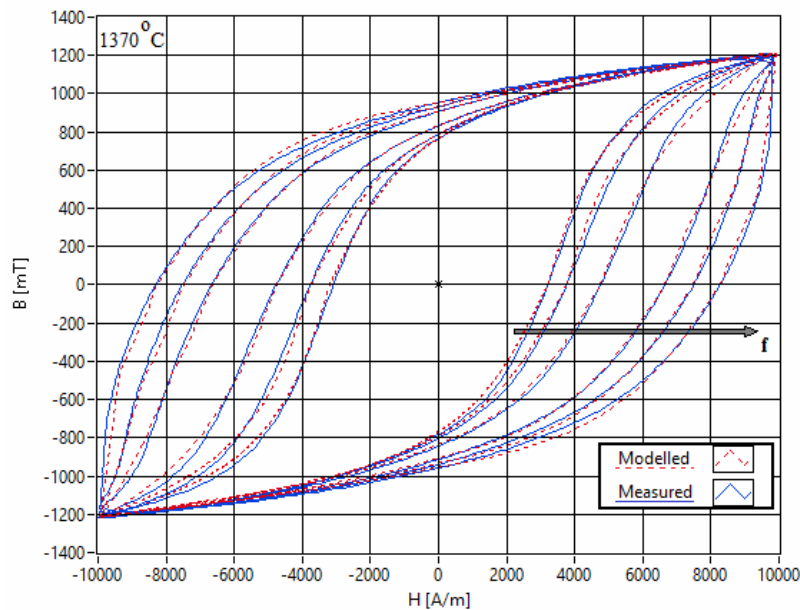


Fig. 8. The B(H) hysteresis loops broadening for FeCo-2V sample sintered at 1370 °C obtained at frequencies of 5 Hz, 10 Hz, 20 Hz, 40 Hz, 50 Hz and 60 Hz ($H_m = 10$ kA/m), measured (line) and modelled (dotted) curves.

4. Conclusion

In this study it was systematically characterized near-equiatomic FeCo-based alloy with addition of 2 wt.% vanadium produced by PIM/MIM technology. Only α -FeCo

crystalline phase is found for all investigated FeCo-2V alloy samples sintered from 1370 °C to 1460 °C in hydrogen atmosphere. Powder particles sintered at the highest temperature 1460 °C were completely melted.

The magnetic hardness and mechanical hardness are in the opposite, i.e. the material with the highest Vickers hardness exhibits the lowest intrinsic coercive force, due to dislocation dimensions. Devices prepared from FeCo-2V alloy are usually exploited under extreme conditions and their functionality is associated with the unique combination of magnetic and mechanical properties. In that sense magnetic measurements were performed in the operating frequency range from 5 Hz to 60 Hz with observed maximum of permeability for sample sintered at 1370 °C ($f = 5$ Hz, $H_{ex} = 3$ kA/m). New mathematical model for simulation of measured dynamic hysteresis loops was successfully applied by LabVIEW software package.

Acknowledgement

This paper reports work undertaken in the context of projects "MagnetoPIM" and OI 172057. MagnetoPIM has been the project supported by the Austrian Federal Funding Agency (FFG) in the course of the programme CIR-CE - Cooperation in Innovation and Research with Central and Eastern Europe, while OI 172057 is financed by the Ministry of Education, Science and Technological Development of the Republic of Serbia.

5. References

1. N. H. Loh, S. B. Tor, K. A. Khor, "Production of metal matrix composite part by powder injection molding", *Journal of Materials Processing Technology*, 108 (2001) 398-407.
2. H. Shokrollahi, K. Janghorban, "Soft magnetic composite materials (SMCs)", *Journal of Materials Processing Technology*, 189 (2007) 1-12.
3. P. Setasuwon, A. Bunchavimonchet, S. Danchavijit, "The effects of binder components in wax/oil systems for metal injection molding", *Journal of Materials Processing Technology*, 196 (2008) 94-100.
4. H. Ye, X. Y. Liu, H. Hong, "Fabrication of metal matrix composites by metal injection molding-A review", *Journal of Materials Processing Technology*, 200 (2008) 12-24.
5. A. Simchi, "Direct laser sintering of metal powders: Mechanism, kinetics and microstructural features", *Materials Science and Engineering: A*, 428 (2006) 148-158.
6. Z. Ebersold, N. Mitrović, S. Đukić, B. Jordović, A. Peulić, "Defectoscopy of direct laser sintered metals by low transmission ultrasonic frequencies", *Science of Sintering*, 44 (2012) 177-185.
7. B. Zlatkov, N. Mitrović, M. V. Nikolić, A. Maričić, H. Danninger, O. Aleksić, E. Halwax, "Properties of MnZn ferrites prepared by powder injection molding technology", *Materials Science and Engineering B-Advanced Functional Solid-state Materials*, 175 (2010) 217-222.
8. A. Silva, J. A. Lozano, R. Machado, J. A. Escobar, P. A. P. Wendhausen, "Study of soft magnetic iron cobalt based alloys processed by powder injection molding", *Journal of Magnetism and Magnetic Materials*, 320 (2008) e393-e396.
9. B. S. Zlatkov, M. V. Nikolić, O. S. Aleksić, H. Danninger, E. Halwax, "A study of magneto-crystalline alignment in sintered barium hexaferrite fabricated by powder

- injection molding”, *Journal of Magnetism and Magnetic Materials*, 321 (2009) 330-335.
10. A. Behvandi, H. Shokrollahi, B. Chitsazan, M. Ghaffari, “Magnetic and structural studies of mechanically alloyed nano-structured $\text{Fe}_{49}\text{Co}_{49}\text{V}_2$ powders”, *Journal of Magnetism and Magnetic Materials*, 322 (2010) 3932–3937.
 11. B. Chitsazan, H. Shokrollahi, A. Behvandi, O. Mirzaee, “Characterization and magnetic coercivity of nanostructured $(\text{Fe}_{50}\text{Co}_{50})_{100-x}\text{V}_{x=0,2,4}$ powders containing a small amount of Co_3V intermetallic obtained by mechanical alloying”, *Powder Technology*, 214 (2011) 105–110.
 12. B. Weidenfeller, M. Anhalt, W. Riehemann, “Variation of magnetic properties of composites filled with soft magnetic FeCoV particles by particle alignment in a magnetic field”, *Journal of Magnetism and Magnetic Materials*, 320 (2008) e362–e365.
 13. Y. Pittini-Yamada, E.A. P’erigo, Y. de Hazan, S. Nakahara, “Permeability of hybrid soft magnetic composites”, *Acta Materialia*, 59 (2011) 4291–4302.
 14. T. Sourmail, “Near equiatomic FeCo alloys: Constitution, mechanical and magnetic properties”, *Progress in Materials Science*, 50 (2005) 816–880.
 15. D. W. Clegg, R. A. Buckley, “The disorder–order transformation in iron–cobalt-based alloys”, *Metal Science Journal*, 7 (1973) 48–54.
 16. G. B. Chon, K. Shinoda, S. Suzuki and B. Jeyadevan, “Order-disorder transformation in $\text{Fe}_{50}\text{Co}_{50}$ particles synthesized by polyol process”, *Materials Transactions* 51 (2010) 707-711.
 17. H. Danninger, Ch. Harold, Ch. Gierl, H. Ponemayr, M. Daxelmueller, F. Simancik and K. Izdinsky, “Powder Metallurgy Manufacturing of Carbon-Free Precipitation Hardened High Speed Steels”, *Acta Physica Polonica A*, 117 (2010) 825-830.
 18. H. Danninger, Ch. Gierl, N. Mitrović, “Magnetic and mechanical properties of sintered Fe-Co-Mo/W precipitation hardened alloys”, Euro PM 2011, Barcelona, October, 2011.
 19. B. D. Cullity, C. D. Graham, “Introduction to magnetic materials”, 2009, IEEE Press, New York.
 20. R. M. Bozorth, “Ferromagnetism”, 1993, IEEE Press, New York.
 21. S. Djukić, V. A. Maričić, A. Kalezić-Glišović, L. Ribić-Zelenović, S. Randjić, N. Mitrović, N. Obradović, “The effect of temperature and frequency on magnetic properties of the $\text{Fe}_{81}\text{B}_{13}\text{Si}_4\text{C}_2$ amorphous alloys”, *Science of Sintering*, 43 (2011) 175-182.
 22. R. Surla, N. Mitrović, S. Djukić, V. Ibrahimović, “Amorphous $\text{Fe}_{72}\text{Cu}_1\text{V}_4\text{Si}_{15}\text{B}_8$ Ribbon as Magneto-Impedance Sensing Element”, *Serbian Journal of Electrical Engineering*, 13 (2016) 381-394.
 23. D. C. Jiles, D. L. Atherton, “Theory of ferromagnetic hysteresis”, *Journal of Magnetism and Magnetic Materials*, 61 (1986) 48-60.
 24. P. Wilson, J. Neil Ross, A. D. Brown, “Simulation of magnetic component models in electric circuits including dynamic thermal effects”, *IEEE Transactions on Magnetics*, 17 (2002) 55 – 65.
 25. S. Cundeva, M. H. J. Bollen, “PSPICE modelling and experimental results of the magnetic behavior of a primary side phase controlled transformer”, *International Conference on Power Systems Transients*, Seattle, USA, June 1997.
 26. A. P. S. Baghel, S. V. Kulkarni, “Dynamic loss inclusion in the Jiles–Atherton (JA) hysteresis model using the original JA approach and the field separation approach”, *IEEE Transactions on Magnetics*, 50 (2014) 369–372.
 27. J. Orelj, N. Mitrović, “Analytical method for hysteresis modelling of magnetic materials applying LabVIEW software package”, to be published.

Садржај: У раду су испитивани торусни узорци легуре FeCo-2V добијени технологијом бризгања композита праха са растопљеним везивом. Бризгање смеше металних прахова са ниско вискозним полимерним везивом омогућава добијање магнетних језгара и у комплексним геометријским облицима. Полазни бризгани узорци су најпре третирани хемијским растварачем а затим и термички третирани ради одстрањивања везива. Високотемпературско синтеровање је спроведено у атмосфери водоника током 3.5 сата у распону температура од 1370 °C до 1460 °C. Испитивање еволуције микроструктуре, микротврдоће и магнетног хистерезиса у функцији температуре синтеровања показало је да најбољу комбинацију функционалних својстава поседује узорак синтерован на температури од 1370 °C. Применом новог математичког модела успешно су спроведене симулације кривих магнетног хистерезиса испитиване у опсегу радних фреквенција од 5 Hz до 60 Hz.

Кључне речи: Технологија бризгања композита праха са растопљеним везивом; легура FeCo-2V; микроструктура; механичка својства; магнетна својства.

© 2016 Authors. Published by the International Institute for the Science of Sintering. This article is an open access article distributed under the terms and conditions of the Creative Commons — Attribution 4.0 International license (<https://creativecommons.org/licenses/by/4.0/>).

